ADAPTIVE COMPLIANCE CONTROL: An Approach to Implicit Force Control in Compliant Motion

Homayoun Seraji
Jet Propulsion Laboratory
California Institute of '1'ethnology
Pasadena, CA 91109

Abstract

This paper addresses the problem of controlling a manipulator in compliant motion while in contact with an environment having an unknown stiffness. Compliance control is used as an ***implicit*** force control scheme and establishes a user-specified target interaction dynamics between the reference position and the contact force. Two adaptive lag-plus- feedfor ward compliance compensators are developed in the paper. The compliance compensators do *not* require force rate information for implementation. Since the environmental stiffness can typically vary by several orders of magnitude, compensator adaptation is used to ensure a stable and uniform system performance. Dynamic simulation results for a 7 1)01" Robotics Research arm are presented to demonstrate the efficacy of the proposed compliance control scheme in executing contact tasks. [1]

1 Introduction

Robust and reliable operation of manipulators in contact with objects in their environment is the basic requirement for successful execution of many robotic tasks. Stable control of robot-environment interaction poses a technically challenging problem, and has attracted the attention of several roboticists for almost two decades [see, e.g., 1-3]. In particular, compliant motion control, which is in essence position-based force control, has been suggested try Kazerooni [4] and Lawrence [5].

The objective of this paper is to develop a simple and pragmatic approach to contact force control using the compliant motion framework. The proposed approach, called ***adaptive compliance control***, is an implicit force control scheme in which the reference position is used as a command to control the contact force, and no force setpoints are used. Two simple adaptive compliance compensators are developed which possess enhanced stability and improved performance under gross variation of the environmental stiffness.

The paper is structured as follows. Section 2 discusses implicit force control within the compliant motion framework. In Section 3, two adaptive lag-plus-feedforward compensators arc developed to accomplish compliance with the environment. In Section 4, the Robotics Research arm is used in a series of dynamic simul at ions to demonstrate compliance control. The paper is concluded in Section 5 with a review and general discussions.

2 Implicit Force Control in Compliant Motion

Robot manipulators arc always supplied with joint servo controllers which ensure tracking of joint setpoints, and, in turn, enable the placement and orientation of their end-effectors in the workspace. For unconstrained free-space motions, the end-effector Cartesian coordinates X (typical] y, a 6x1 vector of position and orientation) can follow a user-spccificd nominal or reference motion trajectory X_r using the joint servos and inverse kinematic transformation. The underlying concept of compliant motion control is to usc the position-controlled robot as a baseline system and to make the necessary modifications to this system to enable execution of constrained tasks that require robot interaction with the environment. Figure 1 shows the block diagram of a position-based implicit force control system when the robot interacts with the environment. The

[1] The research described in this paper was carried out at the Jet Propulsion Laboratory, California Institute of Technology, under contract with the National Aeronautics and Space Administration.

contact force F is fed back to the compliance compensator $K(s)$ which produces the position perturbation X_f, so that the end-effecter tracks the modified commanded trajectory $X_c = X_r - Xl$.

Now, since the manipulator position control system ensures Cartesian trajectory tracking, it can be assumed that the internal position controller, in effect, decouples the robot dynamics. As a result, we can consider each cnd-effecter coordinate independent] y and replace the position/orientation vector X in the control diagram by the scalar x, which can represent any element of X. Furthermore, following Kazerooni [4], Lawrence [5], and other researchers, it is reasonable to model each position-controlled end-effector coordinate by a second-order linear continuous-time system, so that for each end-effecter coordinate the scalar transfer-function relating the commanded position x_c to the actual position z is given by

$$G(s) \quad \frac{..42}{xc(s)} = \frac{K_m}{J_m s^2 + B_m s + K_m} = \frac{b}{s^2 + as + b} \tag{1}$$

where J_m, B_m, and K_m are the position-controlled manipulator mass, damping and stiffness parameters in Cartesian-space respectively, a = $\frac{B_m}{J_m}$ and $b = \frac{K_m}{J_m}$. This simple model can adequately account for the small t ime-delays involved in the forward and inverse kinematic calculations as well as the dynamics of the position-controlled joint servo loops. This model is particularly suitable for industrial robots that use high gear ratios which attenuate the nonlinear manipulator dynami cs and make the second-order joint motor dynamics dominant [6].

The environment can often be modeled as a linear spring with coefficient of stiffness K_{en} along the Cartesian axis of interest. Therefore, the force-displacement model for the environment is given by Hooke's law as

$$F = K_{en}(x - x_e) \tag{2}$$

where x_e is the nominal position of the environment. Similarly, the force/torque sensor mounted on the end-effector can be modeled as a pure spring with the stiffness coefficient K_{sn}, since the dynamics of the sensor can be neglected in comparison with the compensator and manipulator time-constants. Therefore, the effective stiffness of the sensor plus the environment in a Cartesian direction is given by, $K_e = (1/K_{en} + 1/K_{sn})^{-1}$. Note that although the manipulator-environment interaction can be modeled in detail as a Higll-order dynamical system [7, 8], the stiffness is often the dominating factor in contact tasks such as assembly, mating, and deburring [5, 9, 10], Furthermore, this simple mode] is mathematically tractable and has been widely adopted by several researchers. It is important to note that when the robot is in contact with the environment, the dynamic model of the position-controlled end-effector coordinate is modified by the environment, due to natural force feedback as

$$J_m\ddot{x} + B_m\dot{x} + K_m x = K_m x_c - K_e x \tag{3}$$

Hence, at contact, the modified transfer-function G(s) takes the form

$$\tilde{G}(s) = \frac{\mathrm{x(s)}}{xc(s)} = \frac{b}{S^2 + as + b'} \tag{4}$$

where $b' = \frac{(K_m + K_e)}{J_m}$.

In the next section, wc develop two compensators based on compliance control to accomplish stable and desirable contact with the environment.

3 Adaptive Compliance Control

In this section, we consider the compliance control system shown in Figure 2 in which the reference position x_r is used as a command to control the contact force F during constrained tasks. This is accomplished by establishing a desirable position-force $(x_r - F)$ relationship through an appropriate choice of the compensator $K(s)$. Compliance control accepts the position command x_r as. input and produces the contact force F as output, and dots not use any force setpoint. This is in contrast to admittance control [2] in which the force sctpoint F_r is commanded to control the contact force F, and the force error e is mapped to the position perturbation x_f.

In subsequent sections, two simple adaptive compliance compensators are presented to accomplish implicit force control.

3.1 Stability-Based Adaptive Compliance Compensator

Consider the implicit force control systcm shown in Figure 2 with the *lag-plus-feedforward* compliance compensator

$$K(s) = k_f + \frac{k}{k_d s + k_s} = \frac{\alpha s + \beta}{k_d s + k_s} \tag{5}$$

where $\alpha = k_f k_d$ and $\beta = k_f k_s + k$. Without loss of generality and to simplify the analysis, the world frame is defined to be on the environment so that x_e = O. The differential equation relating the contact force F to the reference position x_r is found to be

$$k_d\frac{d^3F}{dt^3} + [k + ak_d]\frac{d^2F}{dt^2} + [ak_s + b'k_d + abk_e]\frac{dF}{dt} + [b'k_s + \beta bk_e]F = [bk_ek_d]\frac{dx_r}{dt} + [bk_ek_s]x_r \tag{6}$$

Now, to apply a constant force on the environment, the reference position x_r will be chosen to penetrate into the environment by a constant amount. Hence, we can set $\frac{dx_r}{dt}$ = O and investigate the stability of the third-order differential equation (6) using a Lyapunov approach. In order to improve the performance of the compliant control system, it is suggested that the compensator gain β be a nonlinear function of the contact force F. On applying Barbashin's theorem to the third-ordcr nonlinear differential equation (6), the following three stability conditions are obtained [1 1]:

(i) $\frac{k_s + ak_d}{k_d} > 0$

(ii) $\frac{b'k_s + bk_e\beta}{k_d} F^2 > 0$

(iii) $\left[\frac{k_s + ak_d}{k_d}\right]\left[\frac{ak_s + b'k_d + ak_eb}{k_d}\right] - \frac{d}{dF}\left[\frac{b'k_s + bk_e\beta}{k_d} F\right] > 0$

where it is assumed that the parameters (k_d, k_s, α) of the compensator are fixed and the parameter β is a function of the contact forc$_e F$. Conditions (i) and (ii) are satisfied when the compensator parameters $(k_d, k_s, \alpha, \beta)$ arc chosen to be positive. Condition (iii) simplifies to

$$\left[\beta + F\frac{d\beta}{dF}\right] < \frac{1}{bk_e}\left[a\frac{k_s^2}{k_d} + ab'k_d + a^2k_s\right] + \left[\alpha a + \alpha\frac{k_s}{k_d}\right] \quad (7)$$

Suppose that wc wish to emulate the user-spccifi'ed steady-state *static* target interaction model

$$F_m = k_m x_{ss} \quad (8)$$

Then, wc can choose the compensator gain β as a function of deviation of the actual contact force F from its desired value F_m. Now, β must be chosen such that $\beta + F\frac{d\beta}{dF}$ has a finite upper-bound which satisfies the stability, inequality (7). A viable choice of β is

$$\beta = \beta_0 + \gamma[1 - exp(F_m - F)/\tau] \quad (9)$$

where γ and$_\tau$ are positive constants specified by the user, and β_0 is the nominal value of β that produces the target model stiffness ***km.*** With this choice of β, when $F > F_m$ the value of β increases, and this in turn decreases the apparent stiffness $k_{ss} = bk_ek_s/[b'k_s + bk_e\beta]$ obtained from (6) and reduces the contact force F. Similarl y, when $F < F_m$, β decreases to increase the apparent stiffness and thus increases the contact force. Note that since $\frac{d\beta}{dF} = \frac{\gamma}{\tau} exp[(F_m - F)/\tau]$, γ reflects the "rate-of-adapt, ation" or sensitivity of/? to ***F.*** It can readily be shown that with this choice of β, the expression $\beta + F\frac{d\beta}{dF}$ is upper-bounded by β_m, that is

$$\beta + F\frac{d\beta}{dF} < \beta_m \quad (lo)$$

where $\beta_m = \beta_0 + \gamma[1 + exp(F_m/\tau - 2)]$. Hence, from inequalities (7) and (10), wc conclude that a *sufficient* condition for closed-loop stability is given by

$$\beta_m < \alpha a + \alpha\frac{k_s}{k_d} \quad (11)$$

A more conservative sufficient, but not a necessary, condition for stability is found to be

$$\frac{\beta_m}{\alpha} < \frac{k_s}{k_d} \quad (12)$$

Inequality (12) imposes a simple condition which guarantees closed-loop stability without any knowledge of the robot parameters (a, b, b') or the environmental stiffness k_e.

In order to appreciate the operation of the compensator gain β, from (9) wc obtain

$$\frac{d\beta}{dt} = \left\{\frac{\gamma}{\tau} exp[(F_m - F)/\tau]\right\} \cdot \frac{dF}{dt} \quad (13)$$

From (13), it is seen that $\frac{d\beta}{dt}$ and $\frac{dF}{dt}$ have the same sign. This implies that when F is increasing $\left(\frac{dF}{dt} > O\right)$, β also increases in order to reduce F to F_m. Similarly, when F is decreasing $\left(\frac{dF}{dt} < O\right)$, β also decreases so as to increase F to F_m. We conclude that the adaptation law given by (9) is expected to improve the performance of the compliant control system.

3.2 MRAC-Based Adaptive Compliance Compensator

Consider the compliant motion control system shown in Figure 2. In this section, we develop a simple MRAC-based adaptive compliance control scheme to ensure that the ***dynamic*** model relating the reference position x_r to the contact force F emulates a user- specified target dynamic model. 'l'his enables the robot to exhibit the same response characteristics, e.g., apparent stiffness and time-constant, when contacting environments with different stiffnesses.

From equation (6), the ***actual interaction dynamics*** representing the manipulator-environment interaction can be described by the third-order differential equation

$$\frac{k_d}{bk_e}\frac{d^3F}{dt^3} + \left[\frac{k_s + ak_d}{bk_e}\right]\frac{d^2F}{dt^2} + \left[\frac{ak_s + b'k_d}{bk_e} + \alpha\right]\frac{dF}{dt} + \left[\frac{b'k_s}{bk_e} + \beta\right]F = k_d\frac{dx_r}{dt} + k_sx_r \quad (14)$$

The numerical value of k_d is often chosen to be small to filter out the high-frequency noise superimposed on the contact force. Furthermore, $\frac{1}{k_e}$ is often a small number

in practice. Therefore, for adaptive control development [12], the third-order full dynamic model (14) can be approximated by the first-order reduced dynamic model

$$\left[\frac{ak_s + \alpha k_d}{bk_e}\right]\dot{F}(t) + \left[\frac{\beta}{bk_e}\right]F(t) = k\dot{x}_r(t) + k_s x_r(t) \qquad (15)$$

Notice that the reduced-order model (15) can alternatively be obtained by ignoring the dynamics of the position-controlled robot. On applying a reference position command x_r with constant final value, the contact force F responds with the time-constant $\tau = \frac{ak_s + b'k_d + bk_e\alpha}{b'k_s + bk_e\beta}$ and presents the steady-state apparent stiffness $k_{ss} = \frac{bk_e k_s}{b'k_s + bk_e\beta}$. It is seen that both the response time and the apparent stiffness are functions of the environmental stiffness k_e. Therefore, during contact with soft environments ($k_e \ll$), $\tau \approx \frac{ak_s + b'k_d}{b'k_s}$ and $k_{ss} \approx 0$; while for hard environments ($k_e \gg$), $\tau \approx \frac{\alpha}{\beta}$ and $k_{ss} \approx \frac{k_s}{\beta}$. Since the environmental stiffness k_e can vary by several orders of magnitude, if the compensator parameters $[\alpha, \beta, k_d, k_s]$ are fixed, the robot will exhibit highly non-uniform and possibly unstable response characteristics when contacting different environments.

In order to overcome this problem and obtain a uniform and desirable performance, a simple adaptive scheme is proposed to "tune" the compensator gains α and β automatically on-line as functions of the contact force F, while choosing constant values for k_d and k_s. In practice, we set $k_s = 1$ and choose k_d to filter out the fen-ce measurement noise. Suppose that the *desired* dynamic performance of the contact force F in response to the reference position x_r is described by the *target interaction dynamics*

$$\frac{\tau_m}{k_m}\dot{F}_m(t) + \frac{1}{k_m}F_m(t) = k\dot{x}_r(t) + k_s x_r(t) \qquad (16)$$

where F_m denotes the desired behavior of F, and τ_m and k_m are the desired user-specified time-constant and apparent stiffness, respectively. This ensures that the environment behaves like a simple spring-damper-spring system with user-specified parameters τ_m, k_m, k_d, and k_s. Following [13], the adaptation laws for $\alpha(t)$ and $\beta(t)$ which ensure that the actual interaction dynamics (15) tends to the target interaction dynamics (16) are given by

$$\alpha(t) = \alpha(0) + \gamma_1 \int_0^t e(t)\dot{F}(t)dt + \gamma_2 e(t)\dot{F}(t) \qquad (17)$$

$$\beta(t) = \beta(0) + \lambda_1 \int_0^t e(t)F(t)dt + \lambda_2 e(t)F(t) \qquad (18)$$

where $e(t) = F(t) - F_m(t)$ is the deviation of the actual contact force $F(t)$ from its desired value $F_m(t)$, $[\gamma_1, \lambda_1]$ are constant positive integral adaptation gains, and $[\gamma_2, \lambda_2]$ are zero or positive constant proportional adaptation gains. The adaptation laws (17)-(18) ensure that the actual contact force F follows the desired contact force F_m asymptotically, i.e., $e(t) \to 0$ as $t \to \infty$. Note that the desired force $F_m(t)$ is obtained by solving the target interaction dynamics (16) with the given reference position $x_r(t)$. To enhance robustness to the unmodeled manipulator dynamics, the a-modification method [12] is used, and the improved adaptation laws are given by

$$\alpha(t) = \alpha(0) + \gamma_1 \int_0^t e(t)\dot{F}(t)dt + \gamma_2 e(t)\dot{F}(t) - \sigma_1 \int_0^t \alpha(t)dt \qquad (19)$$

$$\beta(t) = \beta(0) + \lambda_1 \int_0^t e(t)F(t)dt + \lambda_2 e(t)F(t) - \sigma_2 \int_0^t \beta(t)dt \qquad (20)$$

The o-modified adaptation laws (19)-(20) for α and β ensure that the residual tracking-error $e = F - F_m$ tends to a bounded set of Order $(\sigma^{\frac{1}{2}})$, while guaranteeing robustness to the unmodelcd third and second-order dynamic terms in equation (14).

Finally, by setting $\gamma_2 = 0$ and using integration-by-parts, equation (19) simplifies to

$$\alpha(t) = \alpha(0) + \tfrac{1}{2}\gamma_1 F^2(t) - \gamma_1 F_m(t)F(t) + \gamma_1 \int_0^t \dot{F}_m(t)F(t)dt - \sigma_1 \int_0^t \alpha(t)dt \qquad (21)$$

Note that since the desired contact force $F_m(t)$ is a smooth noise-free signal obtained from the target interaction model (16), the desired force rate $\dot{F}_m(t)$ can be computed directly and used in the adaptation law (21). It is seen that the computation of the compensator gain $\alpha(t)$ from equation (21) does not require knowledge of the actual force rate $\dot{F}(t)$, which can be difficult to obtain in practice since $F(t)$ is a noisy signal.

We conclude that the adaptive lag-plus-feedforward compliance control law is given by

$$x_f(t) = \frac{1}{k_d}\alpha(t)F(t) + [P(t) - \frac{k_s}{k_d}\alpha(t)]\hat{F}(t) \qquad (22)$$

where $\hat{F} = \frac{1}{k_d s + k_s}F$ is the filtered contact force, and the control scheme is shown in Figure 3. ***Notice that neither the compliance control law (22) nor the adaptation laws (20)-(21) require the contact force rate information $\dot{F}(t)$.***

4 Simulation Study

The force control scheme described in Section 3 is now applied through computer simulations to the 7

DOF Robotics Research Corporation (RRC) Model K-1607 arm, shown in Figure 4. The full nonlinear dynamic model for this arm is integrated into a graphics-based robot simulation environment hosted on a Silicon Graphics Personal IRIS workstation [14]. In the simulation, the robot position control system employs a high-performance adaptive controller described in [15]. This controller ensures that any commanded end-effecter position trajectory x_c is tracked accurate] y.

The simulation study demonstrates the capability of the proposed compliance control scheme to achieve a desired end-effecter/environment contact force. In this study, a frictionless reaction surface modeled as linearly elastic with a stiffness of 100lb./in in series with a damper having the friction coefficient of 10lb.sec./in is placed in the robot workspace. This reaction surface is oriented normal to the y axis and is located at $y_e = -22.125$; thus the measured contact force F is modeled as

$$F = \begin{cases} 0 & \text{if } y \leq -22.125 \\ 100(y + 22.125) + 10\dot{y} & \text{if } y > -22.125 \end{cases}$$

The task requires the exertion of a 10lb contact force normal to the reaction surface while tracking a smooth 5in trajectory tangent to the surface. Thus we define $x_r = x_i + 2.5[1 - \cos(\pi/5)t]$ for $t \in [0, 5]$, where x_i is the x component of the initial end-effecter position. For simplicity, the end-effecter orient ation and z coordinate are maintained at their initial values throughout the t ask,

To illustrate robustness of the force control scheme in accommodating unexpected changes in the environmental stiffness, the stiffness k_e is changed abruptly from $k_e = 1001b/in$ to $k_e = 25lb/in$ at the midpoint of the x_r trajectory at $t = 2.5$ seconds. The control objective is to maintain the contact force at 10lb despite this stiffness variation. This situation can occur in practice when tracking along a surface composed of two materials with different stiffness.

Let us apply the MRAC-based adaptive lag-plus-feedforward compliance compensator $K(s) = \frac{\alpha s + \beta}{k_d s + k_s}$ developed in Section 3.2, where α and β are adap tive gains while k_d and k_s are fixed coefficients set at $k_d = 0.05$, and $k_s = 1$. With this choice of (k_d, k_s), the cutoff frequency of the low-pass filter $\frac{1}{k_d s + k_s}$ is at 20rad/sec. For compliance control, there is no force setpoint F_r; instead the desired *contact* dynamics is specified by the user. Suppose that the target contact dynamics is chosen as

$$0.004\dot{F}_m(t) + 0.02F_m(t) = 0.05\dot{y}_r(t) + y_r(t) \qquad (23)$$

which has the desired time-constant $\tau_m = \frac{0.004}{0.02} = 0.2$ scc and the desired stiffness $k_m = \frac{1}{0.02} = 50lb/in$. To obtain a constant contact force of 10lb, the reference position is chosen to penetrate into the reaction surface by $y_r = 0.2$ inches, so that $F_{ss} = k_m y_r = (50)(0.2) = 10lb$. The adaptation laws for the compensator gains α and β are chosen as

$$\alpha(t) = 10^{-4}\left\{0.1 + 0.001 \int_0^t e(t)\dot{F}(t)dt - \int_0^t \alpha(t)dt\right\} \qquad (24)$$

$$\beta(t) = 10^{-4}\left\{0.1 + 10\int_0^t e(t)F(t)dt - \int_0^t \beta(t)dt\right\}$$

where $e(t) = F(t) - Fro(t)$, and $Fro(t)$ is obtained by solving the target dynamics (23) with $y_r = 0.2$. Figures 5a and 5b depict the variations of the contact force F and the compensator gain β during the task.[2] From Figure 5a, it is seen that initially the contact force F responds rapidly to the step reference position y_r. This initial deviation of F from F_m causes the adaptive gain β to increase, which in turn forces F to track the desired trajectory F_m. The transient response lasts $5\tau_m = 1$ second and fort > 1, F tracks F_m exactly and reaches the steady-state value $F_{ss} = k_m y_r = 10lb$. At $t = 2.5$ scc when the environmental stiffnes k_e decreases abruptly, the contact force drops instantaneously but is restored to the target force F_m in 1.5 seconds. Since β determines the stiffness of the compensator as given by $k_c = K^{-1}(0) = \frac{k_s}{\beta} = \beta^{-1}$, it is interesting to consider the steady-state values of β in the time periods $0 < t < 2.5$ and $2.5 < t < 5$. During contact with the hard surface ($k_e = 100$), from Figure 5b we have $\beta_{ss} = 0.01$; hence $k_c = 100$ and the apparent stiffness is $k_{ap} = [k_c^{-1} + k_e^{-1}]^{-1} = [0.01 + 0.01]^{-1} = 50$ which is the specified model stiffness k_m. During contact with the soft surface ($k_e = 25$), from Figure 5b wc have $\beta_{ss} = -0.02$; hence $k_c = -50$ and $k_{ap} = [-0.02 + 0.04]^{-1} = 50 = k_m$ again. We conclude that the adaptation law has resulted in a *negative* value for β [corresponding to positive force feedback loop] in order to *increase* the apparent stiffness of the surface from $k_e = 25$ to $k_m = 50$. Finally, note that from Section 3.2 the force rate information F is *not* required for implementation of this control scheme.

5 Discussions and Conclusions

Force control based on compliant motion is discussed in this paper. The compliance control approach is an implicit force control scheme that uses reference position as command and achieves a desired contact dynamics. The adaptive compensator gains ensure stable and uni-

[2] Since the adaptation gain for α is small, α varies very slightly from its initial value.

form performance in contact with environments having unknown stiffnesses.

It is important to appreciate the subtle difference between the conventional impedance control and the proposed compliance control. Consider the standard second-order target impedance dynamics [3]

$$m\ddot{x}_r + b[\dot{x}_r - \dot{x}] + k[x_r - x] = F$$

where x_r is the reference position and x is the actual position of the cnd-effecter and F is the contact force. Assuming a linearly elastic environment, $F = k_e x$, the impedance dynamics reduces to

$$\frac{b}{k_e}\dot{F} + \left(1 + \frac{k}{k_e}\right)F = m\ddot{x}_r + b\dot{x}_r + kx_r$$

It is seen that the dynamic model relating x_r to F is ***dependent*** on the environmental stiffness k_e. Hence, under impedance control, the robot will exhibit different characteristics, e.g., apparent stiffness and response time, when contacting different environments. This is in contrast to the proposed compliance control approach which attempts to maintain a user-specified invariant target dynamics between x_r and F *irrespective* of the environmental stiffness, such as

$$\frac{\tau_m}{k_m}\dot{F}_m(t) + \frac{1}{k_m}F_m(t) = k_d\dot{x}_r(t) + k_s x_r(t)$$

where τ_m, k_m, k_d, and k_s are user-specified parameters. Hence, the goal of compliance control is to provide the same robot-environment interactoin dynamics regardless of the environmental stiffness.

References

[1] D. E. Whitney: "Force Feedback Control of Manipulator Fine Motions," ASME Journal of Dynamic System's, Measurement, and Control,. pp. 91-97, 1977.

[2] M. Raibert and J. Craig: "Hybrid Position/Force Control of Manipulators", ASME Journal of Dynamic Systems, Measurement, and Control, Vol. 102, No. 2, pp. 126-133, 1981.

[3] N. Hogan: "Impedance Control: An Approach to Manipulation, Parts I-III", ASME Journal of Dynamic Systems, Measurement, and Control, Vol. 107, No. 1, pp. 1-24, 1985.

[4] H. Kazerooni, B. J. Waibel, and S. Kim: "On the Stability of Robot Compliant Motion Control," ASME Journal of Dynamic Systems, Measurement, and Control, Vol. 112, pp. 417-426, 1990.

[5] D. A. Lawrence and R. M. Stoughton: "Position-Based Impedance Control: Achieving Stability in Practice," Proc. AIAA Guidance, Navigation, and Control Conference, pp. 221-226, Monterey, 1987.

[6] M. C. Good, L. M. Sweet, and K. L. Strobe]: "Dynamic Models for Control System Design of Integrated Robot and Drive Systems," ASME Journal of Dynamic Systems, Measurement, and Control, Vol. 107, pp. 53-59, 1985.

[7] R. A. Volpe: "Real and Artificial Forces in the Control of Manipulators: Theory and Experiments," Ph.D. dissertation, Carnegie-Mellon University, 1990.

[8] S. D. Eppinger and W. P. Seering: "On Dynamic Models of Robot Force Control," Proc. IEEE International Conference on Robotics and Automation, Vol. 1, pp. 29-34, San Francisco, 1986.

[9] H. Ishikawa, C. Sawada, K. Kawase, and M. Takata: "Stable Compliance Control and its Implementation for a 6 DOF Manipulator," Proc. IEEE International Conference on Robotics and Automation, pp. 98-103, Scottsdale, 1989.

[10] 0. Khatib and J. Burdick: "Motion and Force Control of Robot Manipulators," Proc. IEEE International Conference on Robotics and Automation, Vol. 3, pp. 1381-1386, San Francisco, 1986.

[11 W. J. Cunningham: "An Introduction to Lyapunov's Second Method/' in 'Work Sessions in Lyapunov's Second Method,' 1,. F. Kazda (Ed.), 1960.

[12] P. A. Ioannou and P. V. Kokotovic: ***Adaptive Systems with Reduced Models,*** Springer-Verlag, New York, 1983.

[13] K. Narendra and A. Annaswamy, ***Stable Adaptive Systems,*** Prentice Hall, Englewood Cliffs, NJ, 1989.

[14] K. Glass and R. Colbaugh, "A Computer Simulation Environment for Manipulator Controller Development," NMSU Internal Publication, 1992.

[15] R. Colbaugh, H. Seraji, and K. Glass: "Direct Adaptive Impedance Control of Robot Manipulators," Journal of Robotic Systems, Vol, 10, No. 2, pp. 217-224, 1993.

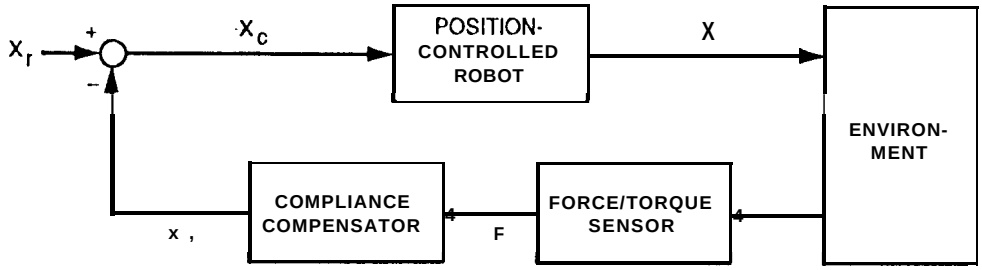

Figure 1. Position-based implicit force control system

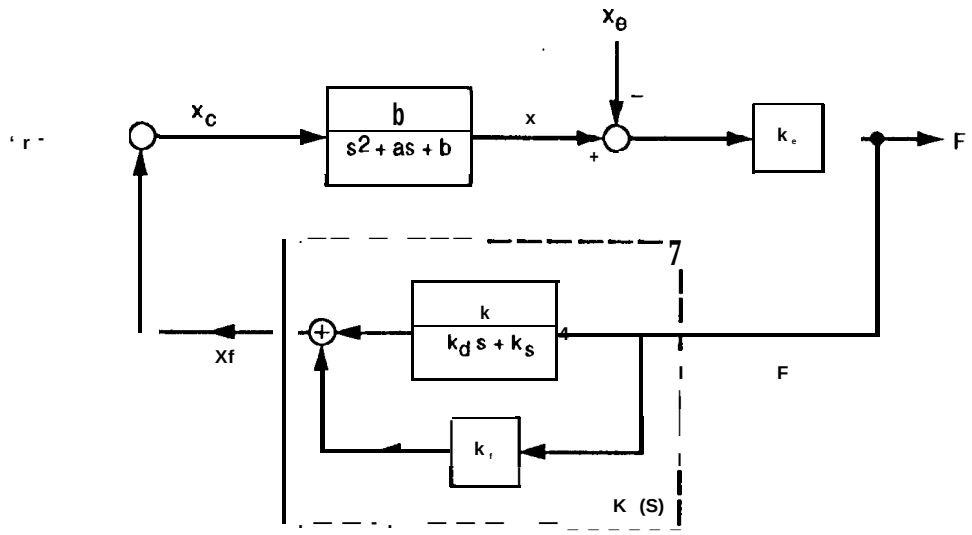

Figure 2. Lag-plus-feedforward compliance control scheme

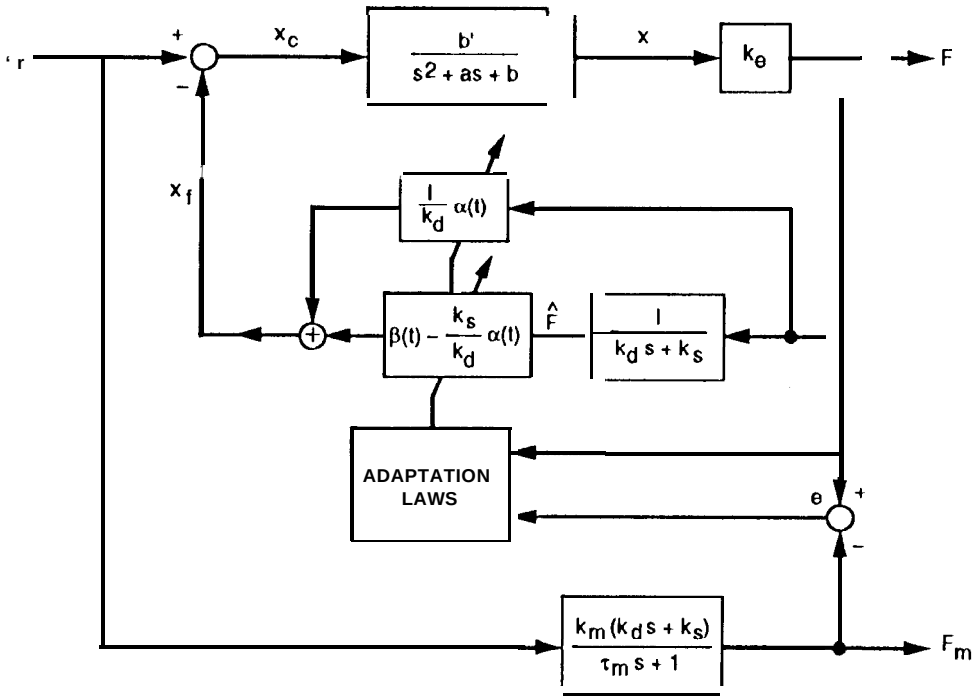

Figure 3. MRAC-based adaptive compliance control scheme

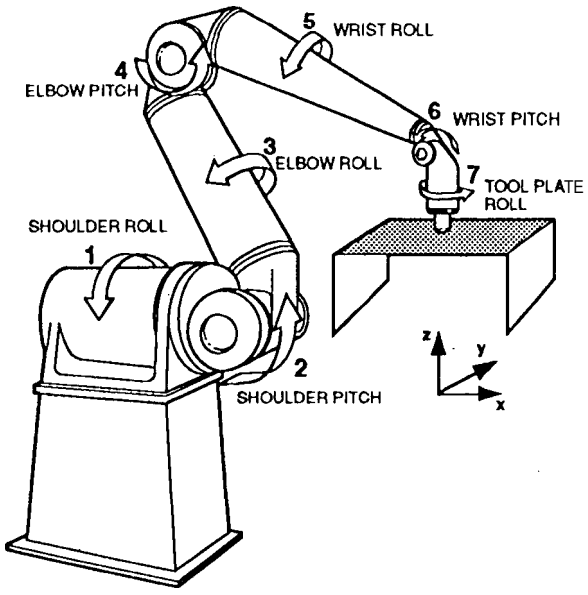

Figure 4. Robotics Research arm in contact with a surface

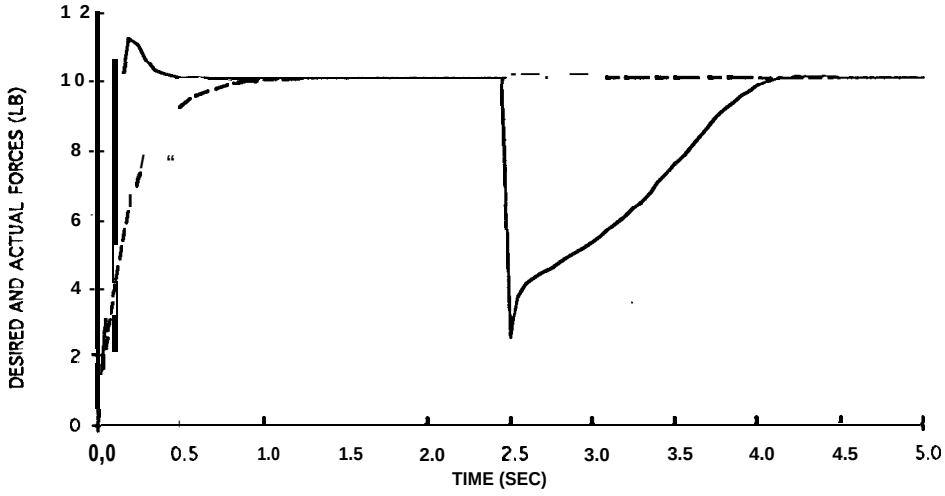

Figure 5a. Variation of the contact force F In the simulation study

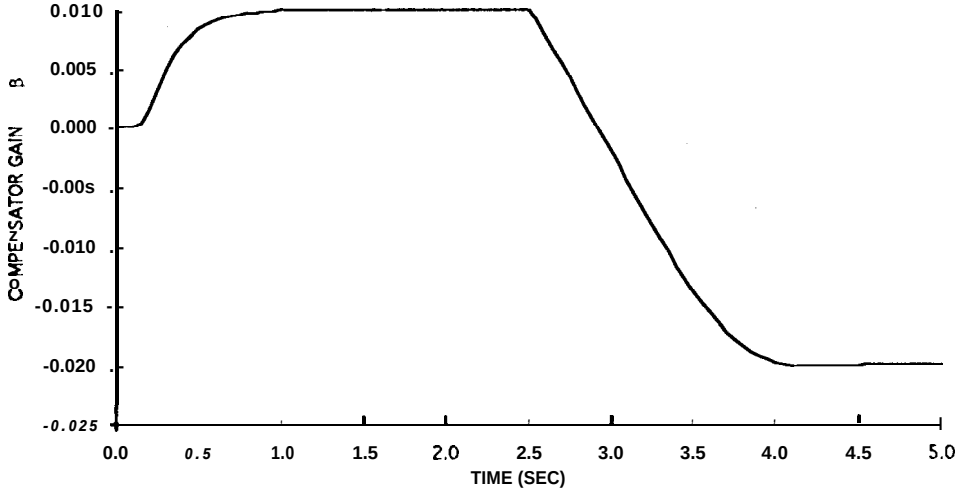

Figure 5b. Variation of the adaptive compensator gain β in the simulation study